

# Entanglement resonance in the asymmetric quantum Rabi model

Yu-Qing Shi,<sup>1,2</sup> Lei Cong,<sup>3,4,\*</sup> and Hans-Peter Eickle<sup>5</sup>

<sup>1</sup>*School of Physical Science and Technology, Lanzhou University, Lanzhou 730000, China*

<sup>2</sup>*College of Electrical Engineering, Northwest Minzu University, Lanzhou 730030, China*

<sup>3</sup>*Department of Applied Physics, Nanjing Tech University, Nanjing 210009, China*

<sup>4</sup>*International Center of Quantum Artificial Intelligence for Science and Technology (QuArtist) and Department of Physics, Shanghai University, 200444 Shanghai, China*

<sup>5</sup>*Humboldt Study Centre, Ulm University, Ulm D-89069, Germany*

We investigate the entanglement features in the interacting system of a quantized optical field and a statically driven two-level atom, known as the asymmetric quantum Rabi model (A-QRM). Intriguing entanglement resonance valleys with the increase of the photon-atom coupling strength and peaks with the increase of the driving amplitude are found. It is revealed that both of the two kinds of entanglement resonance are caused by the avoided level crossing of the associated eigenenergies. In sharp contrast to the quantum Rabi model, the entanglement of the A-QRM collapses to zero in the strong coupling regime except that the driving amplitude equals to  $m\omega/2$ , with  $m$  being an integer and  $\omega$  being the photon frequency. Our analysis demonstrates that such entanglement reappearance is induced by the hidden symmetry of the A-QRM. Supplying an insightful understanding on the A-QRM, our result is helpful in exploring the hidden symmetry and in preparing photon-atom entanglement in light-matter coupled system.

## I. INTRODUCTION

A fundamental model that describes light-matter interaction known as the quantum Rabi model (QRM) [1] reveals the interaction of the atom and the a quantized electromagnetic field. This model plays an important role in modern physics, ranging from quantum optics [2, 3], condensed matter physics [4], quantum information [5, 6], quantum computation [7] and quantum communication [8]. In the field of quantum optics, this model has been realized in many quantum systems [2, 3, 9], such as cavity quantum electrodynamic systems (QED) [10] and circuit-QED [11–15], trapped ions [16–19], photonic system [20], and quantum dots [21–23]. These advanced quantum technologies have enabled ultra-strong [24–26] or deep strong coupling regimes [27] of photon-atom interactions. In the meanwhile, the theoretical research of the full QRM has been boosted [28], characterized by the analytical solution [29–35] and few-body quantum phase transition [36] with experiment confirmation [37] and further application in quantum metrology [38] and the generations of QRM [39–41] and so on.

Among the generations, the asymmetric quantum Rabi model (A-QRM) has attracted much attention recently [42–46]. The A-QRM contains an extra driving term  $\epsilon\sigma_x$  compare to the standard QRM [29]. It is a pretty much useful model, in reality, this model could be dated back to 2002 that Armour *et al.*[47] proposed the model of a micromechanical resonator coupled to a Cooper-pair box with the purpose of probing the quantum entanglement and 2003 that Irish *et al.* proposed for quantum measurement [48]. Besides, it has been designed to be a quantum coherent heat engine [49].

In theoretical research, the extra driving term was first introduced to break the  $\mathbb{Z}_2$  symmetry of QRM [29]. The interesting thing is that A-QRM seems to recover the symmetry at some certain values of  $\epsilon$  [29, 42, 50, 51]. Many scholars found that the A-QRM has a hidden symmetry [42–45]. More recently, an analysis of the energy spectrum of the A-QRM from a numerical point of view reveals that the hidden symmetry manifesting the energy level crossover happens for the driving amplitude  $\epsilon$  equaling to an integer times half of the photon frequency  $\omega$  [46]. However, sometimes it is trouble to distinguish the level crossing and anti-level crossing. Thus, a physical quantity that provides a more intuitive understanding of the structure of the energy spectrum will be very helpful. Besides, the level crossing happens in the mediate coupling regime, is there any physical features related to the hidden symmetry in the stronger coupling regime?

In this work, we investigate the entanglement properties of the eigenstates of the A-QRM. Reflecting the non-locality nature of quantum physics, entanglement has been seen as a basic resource in quantum technology [52]. It also has been applied to study the level crossing in anisotropic QRM [39], spectral classification [53], and quantum phase transition in the QRM [54]. Here, by studying the entanglement of the eigenstates of the A-QRM in different coupling strengths and driving amplitudes, we find that the entanglement is sensitive to the energy-spectrum feature. Explicitly, the entanglement exhibits distinctive resonance valleys with the increase of the coupling strength and resonance peaks with the increase of the driving amplitude, both of which are caused by the avoided level crossing of the associated eigenstates. Note that the similar entanglement resonance behavior has been discussed earlier in spins chains [55] and periodically driven multi-partite quantum systems [56]. We also uncover that the entanglement reappearance in the strong photon-atom coupling regime when  $\epsilon = m\omega/2$  is

\* [conglzu@gmail.com](mailto:conglzu@gmail.com)

guaranteed by the hidden symmetry of the A-QRM. Serving as an obvious evidence to reflect the hidden symmetry, our result supplies insightful understanding on the physics of the A-QRM.

This paper is outlined as follows. In Sec II, we give the Hamiltonian and the entanglement characterization of the A-QRM. The entanglement resonance with the increase of the photon-atom coupling strength is also revealed. In Sec. III, we study the entanglement resonance with the increase of the driving amplitude. The entanglement preservation caused by the hidden symmetry is also uncovered. Finally, we give a summary in Sec. IV .

## II. THE MODEL AND ENTANGLEMENT RESONANCE

We consider the A-QRM, which describes the interaction between a quantized optical field and a static-field driven two-level atom. Its Hamiltonian reads

$$\hat{H} = \omega_0 \hat{\sigma}_+ \hat{\sigma}_- + \omega \hat{a}^\dagger \hat{a} + [g(\hat{a}^\dagger + \hat{a}) + \epsilon](\hat{\sigma}_+ + \hat{\sigma}_-), \quad (1)$$

where  $\hat{a}$  is annihilation operator of the optical field with frequency  $\omega$ ,  $\hat{\sigma}_+ = \hat{\sigma}_-^\dagger = |e\rangle\langle g|$  is the transition operator between the ground state  $|g\rangle$  and the excited state  $|e\rangle$  of the atom with frequency  $\omega_0$ ,  $g$  is the atom-field coupling strength, and  $\epsilon$  is the amplitude of static driving [57].

The atom-field entanglement in any eigenstate  $|\Psi\rangle$  of the A-QRM can be quantified by the entanglement entropy. It equals to the von Neumann entropy of the reduced density matrix for any one of the subsystems [52, 58–60],

$$S = -\text{Tr}(\rho_a \log_2 \rho_a) = -\text{Tr}(\rho_f \log_2 \rho_f), \quad (2)$$

where  $\rho_a = \text{Tr}_f(|\Psi\rangle\langle\Psi|)$  and  $\rho_f = \text{Tr}_a(|\Psi\rangle\langle\Psi|)$ . The entanglement entropy equals to zero for a separable state and one for a maximally entangled states.

Expanding the Hamiltonian (1) in the complete basis of the combined system of the atom and the field, we can obtain its matrix representation. It is noted that the rank of the matrix is infinite because Eq. (1) possesses no symmetry. The eigen solutions are numerically obtained by truncating the basis of the matrix to the photon number such that the obtained magnitudes of the eigenenergies converge. We present in Fig. 1 the entanglement entropy of different eigenstates  $|\Psi_n\rangle$  of the A-QRM and the QRM as a function of the atom-field coupling strength. The eigenstate corresponding to the  $n$ -th energy level from low to high is labeled by  $n$ . According to the classification rule proposed in Ref. [53] for  $\epsilon = 0$ , the coupling regimes of the QRM can be classified into the perturbative ultrastrong coupling (pUSC), the nonperturbative ultrastrong–deep strong coupling (npUSC–npDSC), and the perturbative deep strong coupling (pDSC) regimes. The regimes of pUSC and npUSC–npDSC are separated by the first energy-level crossing point and the ones of npUSC–npDSC and pDSC are separated by the energy-level coalescence point. It is interesting to find from Fig.

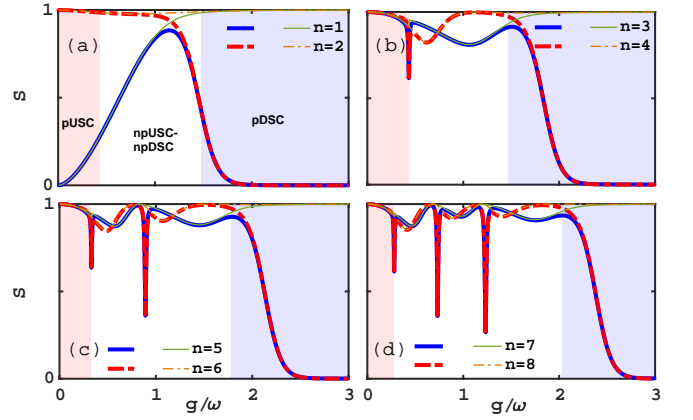


FIG. 1. Entanglement entropy of different eigenstates  $|\Psi_n\rangle$  of the A-QRM with  $\epsilon = 0.01\omega$  denoted by thick lines when  $n = 1, 2$  in (a),  $3, 4$  in (b),  $5, 6$  in (c), and  $7, 8$  in (d) as a function of atom-field coupling strength  $g$ . The corresponding thin lines denote the results of QRM with  $\epsilon = 0$ . Different colors from left to right denote the pUSC, the npUSC–npDSC, and the pDSC regimes, respectively. We use  $\omega_0 = \omega$ .

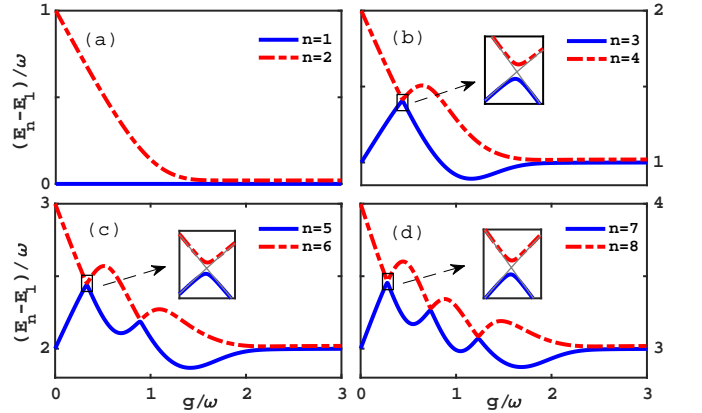


FIG. 2. Eigenenergies corresponding to the A-QRM in Fig. 1 relative to the ground state energy  $E_1$ . The gray solid lines in each inset are the eigenenergies of the QRM with  $\epsilon = 0$ . The places of entanglement resonance in the npUSC–npDSC regime exactly match the ones at which the associated eigenenergies shows avoided level crossing.

1 that, in sharp contrast to the case of QRM with  $\epsilon = 0$ , the entanglement entropy in our A-QRM shows a number of resonance valleys in the npUSC–npDSC regime. It can be estimated that the number of the resonance valleys in this weak driving case equals to  $\lfloor (n-1)/2 \rfloor$ , which matches exactly with the one of the energy-level crossing point in the original QRM [31]. Another remarkable difference of our A-QRM from the conventional QRM is that the entanglement entropy in our A-QRM exclusively decays to zero with the increase of the coupling strength  $g$ , while the corresponding one in the QRM preserves to be one in the pDSC regime.

The entanglement resonance signifies the efficient coupling of the relevant quantum states, which is essentially

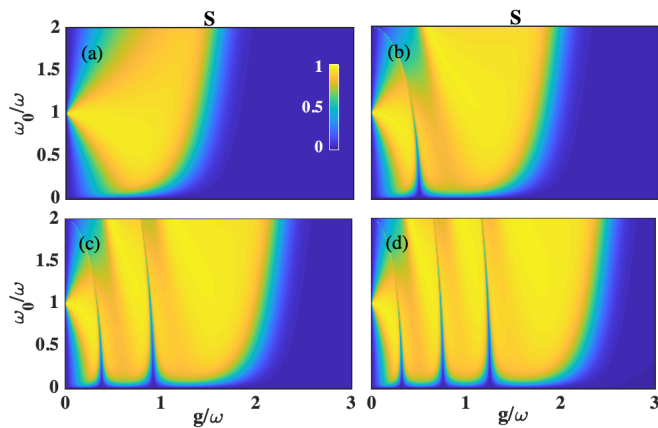


FIG. 3. Entanglement resonance of the eigenstates  $|\Psi_n\rangle$  of the A-QRM in the parameter plane of  $\omega_0$  and  $g$  when  $n = 1$  in (a), 3 in (b), 5 in (c), and 7 in (d). We use  $\epsilon = 0.1\omega$ .

determined by the energy spectrum of the system. To understand the physical reason for the presence of the entanglement resonance in the npUSC-npDSC regime, we plot in Fig. 2 the corresponding energy spectrum of the A-QRM. We can see that all the energy-level crossings in the original QRM is opened by the static driving in the A-QRM. It is interesting to find that the places of the avoided level crossing in Fig. 2 exactly match the ones of entanglement crossing in Fig. 1. It can be physically understood as follows. The application of the static driving makes the  $\mathbb{Z}_2$  symmetry of the original QRM broken and causes its parity  $\exp[i\pi(\hat{\sigma}_+\hat{\sigma}_- + \hat{a}^\dagger\hat{a})]$  nonconserved. It results in the opening of the energy-level crossing of the QRM. At the points of avoided level crossing, the high mixing of the two associated levels with different parities causes an abrupt change to the entanglement of two involved quantum states.

To give a global picture on the entanglement resonance induced by the static driving, we plot in Fig. 3 the entanglement entropy in  $\omega_0$ - $g$  plane for a chosen driving amplitude  $\epsilon$ . It can be seen that the entanglement in the weak-coupling limit is almost zero except for the resonance case  $\omega_0 = \omega$ . Then it changes to one with the tiny increase of  $g$ . With the further increase of  $g$  to the npUSC-npDSC regime,  $\lfloor(n-1)/2\rfloor$  entanglement resonance valleys appears. The entanglement in the small- $\omega_0$  limit equals to zero. It abruptly jumps to one with the increase of  $\omega_0$  except for the entanglement resonance position. Such resonance valleys becomes sharper and sharper with the increase of  $\omega_0$ . Confirming the entanglement resonance induced by the avoided level crossing, the result suggests a useful way to understand the energy-spectrum feature of the quantum-Rabi-family models by monitoring the entanglement between the atom and the quantized field.

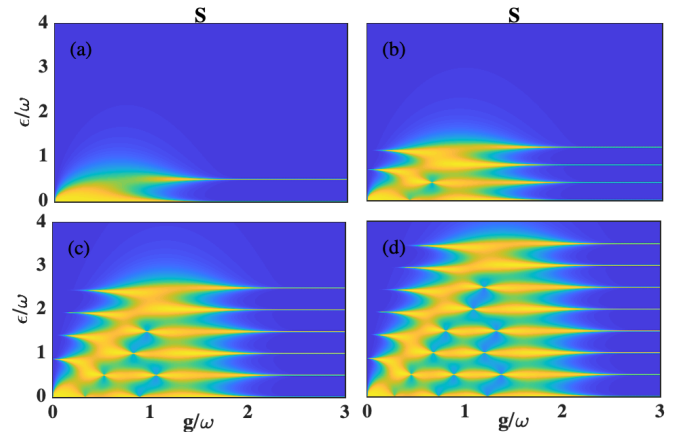


FIG. 4. Entanglement preservation of the eigenstates  $|\Psi_n\rangle$  of the A-QRM when  $\epsilon = m\omega/2$  with  $m \in \mathbb{Z}$ . Here  $n = 2$  in (a), 4 in (b), 6 in (c), and 8 in (d).

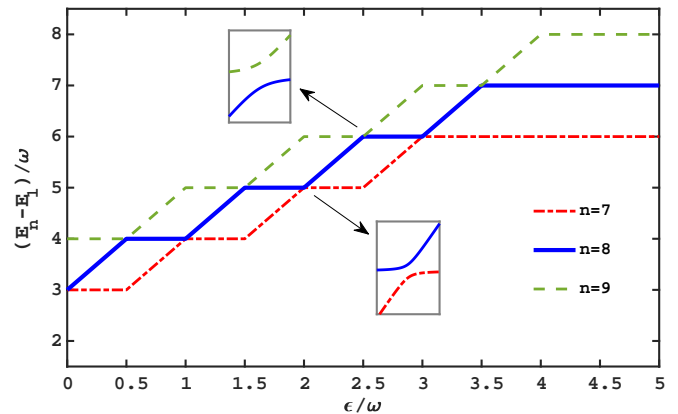


FIG. 5. Eigenenergies relative to the ground state energy  $E_1$  of the A-QRM as a function of the driving amplitude  $\epsilon$  in the pDSC regime when  $g = 3\omega$ . We use  $\omega_0 = \omega$ .

### III. ENTANGLEMENT PRESERVATION IN THE PDSC REGIME

We have seen from Fig. 1 that the entanglement is not preserved in the pDSC regime when a static field is applied. Is this valid for arbitrary  $\epsilon$ ? To answer this question, we explore the entanglement property of the eigenstates  $|\Psi_n\rangle$  of the A-QRM as the change of  $\epsilon$ . In Fig. 4, we present the entanglement entropy of  $|\Psi_n\rangle$  as a function of driving amplitude  $\epsilon$  as well as the coupling strength  $g$  for  $n = 2, 4, 6$ , and 8. It is revealed that, besides the repeated resonance valleys in the npUSC-npDSC regime, which have been analyzed in the last section, the entanglement in the pDSC regime also shows periodic resonance with the increase of  $\epsilon$ . Different from the resonance valleys with the increase of  $g$  in the npUSC-npDSC regime, the entanglement resonance with the increase of  $\epsilon$  in the pDSC regime shows periodic peaks. A maximal entanglement is kept in the pDSC regime at the discrete values  $\epsilon = m\omega/2$ , with  $m$  being an integer. As  $\epsilon$

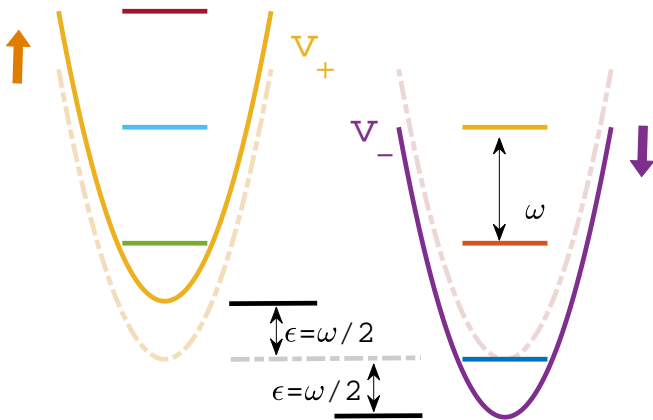


FIG. 6. Schematic diagram of the two harmonic potentials  $V_{\pm}$  associated to the two  $\hat{\sigma}_x$ -eigenstates of  $\hat{H}_0$ . The static driving  $\epsilon$  leads to the upward and downward shifts of  $V_+$  and  $V_-$ , respectively. Here  $\epsilon = \omega/2$  is shown as an example.

further increases, the entanglement disappears again.

The appearance of the entanglement preservation in the pDSC regime when  $\epsilon = m\omega/2$  is also caused by the avoided energy-level crossing. Taking  $n = 8$  as an example, we plot in Fig. 5 the eighth eigenenergy and its nearest-neighbour energies as a function of  $\epsilon$  when  $g = 3\omega$ . It is interesting to observe that the eighth energy level has eight avoided level crossings with its nearest-neighbour levels, which all occur at  $\epsilon = m\omega/2$ . These avoided level crossing corresponds exactly to the entanglement preservation in Fig. 4(d). The result confirms that the entanglement preservation in the pDSC regime when  $\epsilon = m\omega/2$  is essentially determined by the avoided level crossing.

It is out of one's expectation to observe in the pDSC regime of the  $\mathbb{Z}_2$ -symmetry broken A-QRM the avoided level crossing, also called energy quasi-degeneracies, which is governed by the  $\mathbb{Z}_2$  symmetry and presents in the QRM. Actually, the reappearance of the energy quasi-degeneracies in the A-QRM is caused by another symmetry in the A-QRM occurring when  $\epsilon = m\omega/2$ . Such symmetry is called the hidden symmetry of the A-QRM [42–46]. Very recently, its symmetry operators for  $m = 1$  and 2 are rigorously derived [44, 61] and a general scheme to obtain the symmetry operators has been proposed [62]. Thus, in addition to the energy-spectrum features which has been paid attention in previous work, see e.g. [46], the entanglement preservation in the pDSC regime revealed in our work could serve as another evidence of the hidden symmetry of the A-QRM.

Another interesting behavior is that the entanglement preservation occurring at  $\epsilon = m\omega/2$  only happens for a finite number of integers  $m$ . In order to have a physical understanding on this behavior, we apply the polaron picture analysis [63–65]. Such picture has been applied to different generations of QRM and here we mainly focus on the potential picture. Expanding Eq. (1) in the complete basis  $\sum_{s_x=\pm} |s_x\rangle\langle s_x| = 1$  of  $\hat{\sigma}_x \equiv \hat{\sigma}_+ + \hat{\sigma}_-$

and introducing the unit-mass coordinate operator  $\hat{x} = (\hat{a} + \hat{a}^\dagger)/\sqrt{2\omega}$  and momentum operator  $\hat{p} = i\sqrt{\omega/2}(\hat{a}^\dagger - \hat{a})$  of the quantized optical field [63, 64], we can rewrite Eq. (1) as  $\hat{H} = \hat{H}_0 + \hat{H}_1$  with

$$\hat{H}_0 = \sum_{s_x=\pm} \hat{h}_{s_x} |s_x\rangle\langle s_x| + \varepsilon_0, \quad (3)$$

$$\hat{H}_1 = \sum_{s_x=\pm} \frac{\omega_0}{2} |s_x\rangle\langle \bar{s}_x|, \quad (4)$$

where  $\bar{s}_x$  means the flipped spin of  $s_x$ ,  $\varepsilon_0 = (\omega_0 - \omega)/2 - g^2/\omega$  is the constant energy, and  $\hat{h}_{s_x} = \hat{p}^2/2 + \hat{V}_{s_x}$  with

$$\hat{V}_{s_x} = \frac{\omega^2}{2} (\hat{x} + x_{s_x})^2 + s_x \epsilon \quad (5)$$

and  $x_{s_x} = \sqrt{2\omega} s_x g/\omega^2$ . Here  $\hat{V}_{s_x}$  are harmonic potentials with  $s_x = \pm$  labeling the two  $\hat{\sigma}_x$  eigenstates. In the pDSC regime, taking  $\hat{H}_1$  as a perturbation, we obtain the leading order of the eigenenergies of  $\hat{H}$  as

$$E_{n,\pm}^{(0)} = n\omega \pm \epsilon. \quad (6)$$

As illustrated in Fig. 5, one can readily see how the driving  $\epsilon$  affects the entanglement between the atom and the field. The dashed lines represent the case of  $\epsilon = 0$ , where  $V_{\pm}$  are degenerate. With the increase of  $\epsilon$ ,  $V_+$  shifts upwardly and  $V_-$  shifts downwardly with the difference of their valleys being  $2\epsilon$ . The eigenenergies  $E_{n,\pm}^{(0)}$  increases or decreases correspondingly. The second energy level  $|-, 2_-\rangle$  in  $V_-$  intercresses with the second energy level  $|+, 2_+\rangle$  and the first one  $|+, 1_+\rangle$  in  $V_+$  when  $\epsilon = 0$  and  $\omega/2$ , respectively. Except for these two values of  $\epsilon$ ,  $|-, 2_-\rangle$  has no chance to intercress with the energy levels in  $V_-$  anymore. Due to the perturbation of  $\hat{H}_1$ , such energy-level crossings are reopened, which causes the sufficient coupling of  $|-, 2_-\rangle$  with  $|+, 2_+\rangle$  and  $|+, 1_+\rangle$ , respectively. This generates a large entanglement between the atom and the photon. It well explains the result in Fig. 5(a) that a finite entanglement for the second energy level is preserved in the pDSC regime only when  $\epsilon = 0$  and  $\omega/2$ . In the same picture, the results in Figs. 5(b), 5(c), and 5(d) that the entanglement preservation can occurs at  $\epsilon = m\omega/2$  only for  $m = 0, \dots, n-1$  can be understood. Thus, such a simple picture provides an intuitive explanation on the avoided level crossing and entanglement preservation in the pDSC regime.

#### IV. CONCLUSIONS

In summary, we have investigated the entanglement features in the eigenstates  $|\Psi_n\rangle$  of the coupled system of a quantized optical field with a statically driven two-level atom, i.e., the A-QRM. The entanglement exhibits interesting features depending on the light-matter coupling strength and the driving amplitude, which are intrinsically related to the energy-spectrum structure of the A-QRM. It is found that the entanglement show  $[(n-1)/2]$

resonance valleys with the change of light-matter coupling strength in the npUSC-npDSC regimes. Our result indicates that this is caused by the avoided level crossing induced by the static field. In the stronger pDSC regime, the entanglement exhibits resonance peaks at  $\epsilon = m\omega/2$ , with  $m = 0, \dots, n-1$ . Our analysis demonstrates that such entanglement preservation is induced by the avoided level crossing due to the hidden symmetry of the A-QRM. Our result is expected to be helpful to identify the feature of the energy spectrum, such as the avoided energy level crossings, and to further explore the related hidden symmetry properties of more theoretical models for

light-matter interaction [66–68].

## ACKNOWLEDGEMENTS

We would like to thank Prof. Jun-Hong An for helpful discussions. This work is supported by the China Postdoctoral Science Foundation (Grant No. 2019M651463) and the National Natural Science Foundation of Gansu Province, China (Grant No. 20JR5RA509).

- 
- [1] I. I. Rabi, *Phys. Rev.* **49**, 324 (1936).
- [2] D. Walls and G. Milburn, *Quantum Optics* (Springer-Verlag, 1994).
- [3] M. Scully and S. Zubairy, *Quantum Optics* (Cambridge University Press, 1997).
- [4] T. Holstein, *Ann. Phys.* **8**, 325 (1959).
- [5] A. Imamoglu, D. D. Awschalom, G. Burkard, D. P. DiVincenzo, D. Loss, M. Sherwin, and A. Small, *Phys. Rev. Lett.* **83**, 4204 (1999).
- [6] M. A. Nielsen and I. L. Chuang, *Quantum computation and quantum information* (Cambridge university press, 2010).
- [7] L. M. Duan and H. J. Kimble, *Phys. Rev. Lett.* **92**, 127902 (2004).
- [8] L. Childress, J. M. Taylor, A. S. Sørensen, and M. D. Lukin, *Phys. Rev. A* **72**, 052330 (2005).
- [9] I. Arrazola, “Design of light-matter interactions for quantum technologies,” (2021), [arXiv:2101.11695 \[quant-ph\]](https://arxiv.org/abs/2101.11695).
- [10] R. Stassi, A. Ridolfo, O. Di Stefano, M. J. Hartmann, and S. Savasta, *Phys. Rev. Lett.* **110**, 243601 (2013).
- [11] H. Mabuchi and A. C. Doherty, *Science* **298**, 1372 (2002).
- [12] A. Wallraff, D. I. Schuster, A. Blais, L. Frunzio, R.-S. Huang, J. Majer, S. Kumar, S. M. Girvin, and R. J. Schoelkopf, *Nature* **431**, 162 (2004).
- [13] T. D. Ladd, P. van Loock, K. Nemoto, W. J. Munro, and Y. Yamamoto, *New J. Phys.* **8**, 184 (2006).
- [14] D. I. Schuster, A. A. Houck, J. A. Schreier, A. Wallraff, J. M. Gambetta, A. Blais, L. Frunzio, J. Majer, B. Johnson, M. H. Devoret, S. M. Girvin, and R. J. Schoelkopf, *Nature* **445**, 515 (2007).
- [15] P. D. Nation, J. R. Johansson, M. P. Blencowe, and F. Nori, *Rev. Mod. Phys.* **84**, 1 (2012).
- [16] D. Leibfried, D. M. Meekhof, B. E. King, C. Monroe, W. M. Itano, and D. J. Wineland, *Phys. Rev. Lett.* **77**, 4281 (1996).
- [17] K. M. Birnbaum, A. Boca, R. Miller, A. D. Boozer, T. E. Northup, and H. J. Kimble, *Nature* **436**, 87 (2005).
- [18] M. L. Cai, Z. D. Liu, W. D. Zhao, Y. K. Wu, Q. X. Mei, Y. Jiang, L. He, X. Zhang, Z. C. Zhou, and L. M. Duan, “Observation of a quantum phase transition in the quantum rabi model with a single trapped ion,” (2021), [arXiv:2102.05409 \[quant-ph\]](https://arxiv.org/abs/2102.05409).
- [19] D. Lv, S. An, Z. Liu, J.-N. Zhang, J. S. Pedernales, L. Lamata, E. Solano, and K. Kim, *Phys. Rev. X* **8**, 021027 (2018).
- [20] A. Crespi, S. Longhi, and R. Osellame, *Phys. Rev. Lett.* **108**, 163601 (2012).
- [21] J. I. Cirac, P. Zoller, H. J. Kimble, and H. Mabuchi, *Phys. Rev. Lett.* **78**, 3221 (1997).
- [22] D. Englund, A. Faraon, I. Fushman, N. Stoltz, P. Petroff, and J. Vučković, *Nature* **450**, 857 (2007).
- [23] M. Orszag, *Quantum Optics: Including Noise Reduction, Trapped Ions, Quantum Trajectories, and Decoherence* (Springer-Verlag, 2000).
- [24] G. Günter, A. A. Anappara, J. Hees, A. Sell, G. Biasiol, L. Sorba, S. De Liberato, C. Ciuti, A. Tredicucci, A. Leitenstorfer, and R. Huber, *Nature* **458**, 178 (2009).
- [25] T. Niemczyk, F. Deppe, H. Huebl, E. P. Menzel, F. Hocke, M. J. Schwarz, J. J. Garcia-Ripoll, D. Zueco, T. Hümmer, E. Solano, A. Marx, and R. Gross, *Nat. Phys.* **6**, 772 (2010).
- [26] P. Forn-Díaz, J. Lisenfeld, D. Marcos, J. J. García-Ripoll, E. Solano, C. J. P. M. Harmans, and J. E. Mooij, *Phys. Rev. Lett.* **105**, 237001 (2010).
- [27] J. Casanova, G. Romero, I. Lizuain, J. J. García-Ripoll, and E. Solano, *Phys. Rev. Lett.* **105**, 263603 (2010).
- [28] A. L. Boité, *Adv. Quant. Tech.* **3**, 1900140 (2020).
- [29] D. Braak, *Phys. Rev. Lett.* **107**, 100401 (2011).
- [30] Q.-H. Chen, C. Wang, S. He, T. Liu, and K.-L. Wang, *Phys. Rev. A* **86**, 023822 (2012).
- [31] H.-P. Eckle and H. Johannesson, *J. Phys. A: Math. Theor.* **50**, 294004 (2017).
- [32] H.-P. Eckle, *Models of Quantum Matter: A First Course on Integrability and the Bethe Ansatz* (Oxford University Press, 2019).
- [33] L. Yu, S. Zhu, Q. Liang, G. Chen, and S. Jia, *Phys. Rev. A* **86**, 015803 (2012).
- [34] A. J. Maciejewski, M. Przybylska, and T. Stachowiak, *Phys. Lett. A* **378**, 3445 (2014).
- [35] Q. Xie, H. Zhong, M. T. Batchelor, and C. Lee, *J. Phys. A: Math. Theor.* **50**, 113001 (2017).
- [36] M.-J. Hwang, R. Puebla, and M. B. Plenio, *Phys. Rev. Lett.* **115**, 180404 (2015).
- [37] M.-L. Cai, Z.-D. Liu, W.-D. Zhao, Y.-K. Wu, Q.-X. Mei, Y. Jiang, L. He, X. Zhang, Z.-C. Zhou, and L.-M. Duan, *Nat. Commun.* **12**, 1126 (2021).
- [38] L. Garbe, M. Bina, A. Keller, M. G. A. Paris, and S. Felicetti, *Phys. Rev. Lett.* **124**, 120504 (2020).
- [39] Q.-T. Xie, S. Cui, J.-P. Cao, L. Amico, and H. Fan, *Phys. Rev. X* **4**, 021046 (2014).

- [40] L. Cong, X.-M. Sun, M. Liu, Z.-J. Ying, and H.-G. Luo, *Phys. Rev. A* **99**, 013815 (2019).
- [41] L. Cong, S. Felicetti, J. Casanova, L. Lamata, E. Solano, and I. Arrazola, *Phys. Rev. A* **101**, 032350 (2020).
- [42] M. Wakayama, *J. Phys. A: Math. Theor.* **50**, aa649b (2017).
- [43] J. Semple and M. Kollar, *J. Phys. A: Math. Theor.* **51**, 044002 (2017).
- [44] V. V. Mangazeev, M. T. Batchelor, and V. V. Bazhanov, *J. Phys. A: Math. Theor.* **54**, 12LT01 (2021).
- [45] Z.-M. Li and M. T. Batchelor, *Phys. Rev. A* **103**, 023719 (2021).
- [46] S. Ashhab, *Phys. Rev. A* **101**, 023808 (2020).
- [47] A. D. Armour, M. P. Blencowe, and K. C. Schwab, *Phys. Rev. Lett.* **88**, 148301 (2002).
- [48] E. K. Irish and K. Schwab, *Phys. Rev. B* **68**, 155311 (2003).
- [49] F. Altintas, A. U. C. Hardal, and O. E. Müstecaphoğlu, *Phys. Rev. A* **91**, 023816 (2015).
- [50] Z.-M. Li, D. Ferri, D. Tilbrook, and M. T. Batchelor, (2021), [arXiv:2007.11969](https://arxiv.org/abs/2007.11969) [quant-ph].
- [51] K. Kimoto, C. Reyes-Bustos, and M. Wakayama, *Inter. Math. Res. Notices* (2020), 10.1093/imrn/rnaa034.
- [52] J. Eisert, M. Cramer, and M. B. Plenio, *Rev. Mod. Phys.* **82**, 277 (2010).
- [53] D. Z. Rossatto, C. J. Villas-Bôas, M. Sanz, and E. Solano, *Phys. Rev. A* **96**, 013849 (2017).
- [54] M. Liu, Z.-J. Ying, J.-H. An, H.-G. Luo, and H.-Q. Lin, *J. Phys. A: Math. Theor.* **50**, 084003 (2017).
- [55] J. Karthik, A. Sharma, and A. Lakshminarayan, *Phys. Rev. A* **75**, 022304 (2007).
- [56] S. Sauer, F. Mintert, C. Gneiting, and A. Buchleitner, *Journal of Physics B: Atomic, Molecular and Optical Physics* **45**, 154011 (2012).
- [57] Z.-J. Ying, *Phys. Rev. A* **103**, 063701 (2021).
- [58] W. K. Wootters, *Quantum Inf. Comput.* **1**, 27 (2001).
- [59] C. H. Bennett, D. P. DiVincenzo, J. A. Smolin, and W. K. Wootters, *Phys. Rev. A* **54**, 3824 (1996).
- [60] C. H. Bennett, H. J. Bernstein, S. Popescu, and B. Schumacher, *Phys. Rev. A* **53**, 2046 (1996).
- [61] C. Reyes-Bustos, D. Braak, and M. Wakayama, *J. Phys. A: Math. Theor.* **54**, 285202 (2021).
- [62] Y.-F. Xie and Q.-H. Chen, “General symmetry operators of the asymmetric quantum rabi model within bogoliubov operator approach,” (2021), [arXiv:2107.08937](https://arxiv.org/abs/2107.08937) [quant-ph].
- [63] Z.-J. Ying, M. Liu, H.-G. Luo, H.-Q. Lin, and J. Q. You, *Phys. Rev. A* **92**, 053823 (2015).
- [64] L. Cong, X.-M. Sun, M. Liu, Z.-J. Ying, and H.-G. Luo, *Phys. Rev. A* **95**, 063803 (2017).
- [65] L. Cong, X.-M. Sun, M. Liu, Z.-J. Ying, and H.-G. Luo, *Phys. Rev. A* **99**, 013815 (2019).
- [66] Y.-F. Xie and Q.-H. Chen, “Double degeneracy associated with hidden symmetries in the asymmetric two-photon rabi model,” (2021), [arXiv:2102.03944](https://arxiv.org/abs/2102.03944) [quant-ph].
- [67] X. Lu, Z.-M. Li, V. V. Mangazeev, and M. T. Batchelor, “Hidden symmetry operators for asymmetric generalised quantum rabi models,” (2021), [arXiv:2104.14164](https://arxiv.org/abs/2104.14164) [quant-ph].
- [68] X. Lu, Z.-M. Li, V. V. Mangazeev, and M. T. Batchelor, “Hidden symmetry in the biased dicke model,” (2021), [arXiv:2103.13730](https://arxiv.org/abs/2103.13730) [quant-ph].